



Research




# Determination of groundwater potential zones on the eastern slope of Mount Cameroon using geospatial techniques and seismoelectric method

Lionel Junior Ngome Njumbe<sup>1,2</sup>  · Anatole Eugene Djieto Lordon<sup>1</sup> · Christopher M. Agyingi<sup>1</sup>

Received: 28 May 2023 / Accepted: 28 July 2023

Published online: 14 August 2023

© The Author(s) 2023  OPEN

## Abstract

In complex hard rock terrain where the population suffers from water scarcity, the use of site-specific single-method surface geophysical surveys to prospect for groundwater is a common practise. However, this has not completely solved the problem of drilling dry wells. To combat this failure, geospatial data and the analytical hierarchy process (AHP) are being used as supporting techniques to increase the chance of success. This study had the aim of generating a groundwater potential zones (GWPZ) map of the complex strato-volcanic terrain of Buea by integrating geospatial techniques, AHP, and the seismoelectric method. Five factors influencing groundwater recharge were used to define the groundwater potential zones. Via the AHP and weighted overlay methods, five classes of groundwater potential zones were delineated: very poor, poor, moderate, good, and very good. More than half of the study area has good to very good groundwater potential. Lastly, the GWPZ model is validated with an iso-conductivity map from a seismoelectric survey and existing static water level data. The iso-conductivity map revealed four main conductivity zones that correlate positively with the GWPZ map. The northwestern part of the study area is characterised by moderate groundwater potential, poor formation conductivity, and dry boreholes. There is an uneven distribution of groundwater and variable water table depth in the area. The results of this study are very encouraging, and the integrated approach used has proven to be efficient in determining groundwater potential zones in complex volcanic terrain.

## Article Highlights

- More than 65% of the study area has good to very good groundwater potential, and these zones include the older basanites and gentle slope regions.
- The conductivities of the Younger and Recent basanites are very low, coinciding with moderate to poor groundwater potential and occurrence.
- The groundwater table of Buea varies immensely, and it is directly proportional to the slope and elevation.

**Keywords** Analytical hierarchy process · Geospatial techniques · Seismoelectric method · Groundwater potential · Volcanic terrain

✉ Lionel Junior Ngome Njumbe, [lionelngome@gmail.com](mailto:lionelngome@gmail.com) | <sup>1</sup>Department of Geology, University of Buea, Buea, Cameroon. <sup>2</sup>Alexander Drilling Company, Limbe, Cameroon.



SN Applied Sciences

(2023) 5:238

| <https://doi.org/10.1007/s42452-023-05458-w>

SN Applied Sciences  
A **SPRINGER NATURE** journal

## 1 Introduction

Inadequate management practises, a lack of national water policies, poor maintenance and deterioration of infrastructure, corruption, and a lack of adequate funding are some of the problems in developing countries that have resulted in water scarcity [1–4]. As a result, the population is now dependent on groundwater as an alternative and most reliable source of potable water. In the absence of springs, the only other access to groundwater is through wells and boreholes. Nevertheless, the global distribution of groundwater is very uneven [5, 6], especially in active volcanic terrains where there is constant deformation and change in landforms. Additionally, the global groundwater table varies extensively [7], even within small regions like Buea. These are some of the causes of dry boreholes and deeper water levels in certain boreholes in Buea.

Buea, the study area, is situated on the active Mount Cameroon volcano and is noted for water scarcity, especially in the upland villages of Bova, Bonakanda, Bokova, Woteva, Ewonda, Bokwango, and Bwassa, with ever expanding populations. To solve this problem, individuals have been extracting groundwater through boreholes. However, even with the practise of site-specific geophysical surveys, there have been drilling failures with many existing dry boreholes. These frequent drilling failures are due to the geological complexity of the volcanic terrain, the lack of detailed geological and hydrogeological studies, and insufficient geophysical data. Geophysical surveys are more effective when used with a good understanding of the geology and hydrogeological conditions of the area to be exploited. Hence, the assessment and zoning of groundwater potential and the planning and management of groundwater resources are fundamental.

In addition to geophysical surveys, geospatial techniques can be used for groundwater exploration [8–10]. Mapping of groundwater potential zones (GWPZ) is a prerequisite to detailed geophysical surveys for borehole placement. To evaluate the groundwater potential of a region and enhance drilling success, researchers around the world use remote sensing and GIS techniques that are time- and cost-effective [8, 9, 11–14]. Groundwater potential can be inferred from many groundwater recharge influencing factors such as lineament density, land cover, land use, drainage density, vegetation, aspect, rainfall, soil type, e.t.c., depending on regional peculiarities [12, 15–18]. These factors are classified and weighted using multi-influencing factors (MIF) and analytic hierarchy process (AHP) methods [8, 12, 19].

To help solve the water scarcity problem in Buea, this study is the first to integrate remote sensing, geospatial

techniques, and geophysical surveys to demarcate the different groundwater potential zones. This was achieved by using factors influencing groundwater recharge potential in the area, which are lithology, slope, drainage density, lineament density and land use. Each thematic map, including lithology, slope, drainage density, lineament density, and land use, provides a firm indication of the occurrence of groundwater and its potential. Further validation of the groundwater potential zones was done using existing springs and boreholes and their static groundwater level data. The results obtained from this study will serve as a guide and tool for siting boreholes and will aid decision-makers and local authorities in future planning projects such as the zoning of new settlements and groundwater resource management.

## 2 Location and geology

Buea is situated on the eastern slope of Mount Cameroon (Fig. 1), which is the highest mountain in West Africa, standing at 4095 m.a.s.l. [20]. It is the capital of Fako Division in the Southwest Region of Cameroon and has a coastal equatorial climate [21], with two major seasons: the dry season and the rainy season. The dry season starts in mid-October and ends in mid-March, while the rainy season goes from mid-March to mid-October. February is the hottest month with an average temperature of 29 °C, and August is the coldest month with an average temperature of 26 °C. The mean annual temperature and precipitation of Buea are 27 °C and 119 mm, respectively, with August being the wettest month with 326.7 mm of precipitation and January the driest with 3.1 mm [22]. The vegetation type in this region is tropical evergreen forest that ranges from primary thick forest, secondary forest, and shrubs to savannah towards the peak of the mountain [23].

The geology of Buea is indicative of that of Mount Cameroon, an active volcano that last erupted in the year 2000 [24, 25]. Mount Cameroon is one of the volcanic centres of the Cameroon Volcanic Line (CVL) that runs from Pagalu Island in the Atlantic Ocean to Lake Chad [26–30]. Mount Cameroon is a stratovolcano that erupts both effusions of mafic lava and strombolian-style explosive lava [24]. The lithology of the Buea is composed of basanites, lahars, trachyte, and trachybasalt [20, 24, 25, 31] (Fig. 1). These rocks show extensive fracturing. The fractures have more or less an N-S orientation.

## 3 Materials and methods

To achieve the main aim of the current study, we followed the procedure indicated in Fig. 2. Remotely sensed data were used to generate thematic maps, which were

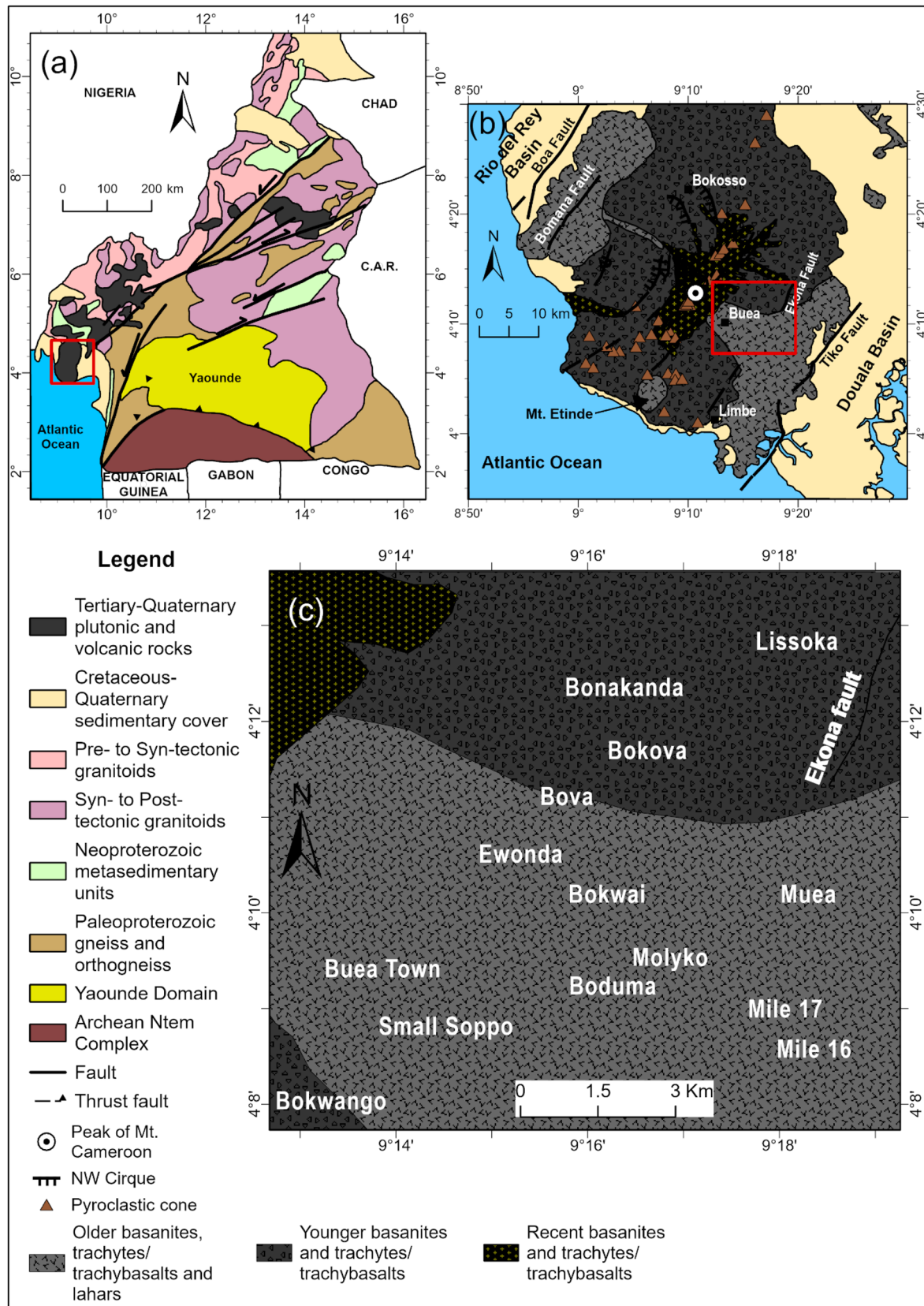


Fig. 1 Geological map of **a** Cameroon, **b** Mount Cameroon [25], **c** study area (adapted from [25])

integrated to produce the GWPZ map. An area of 12 km by 11 km in Buea was selected for the case study. Field verification and validation of the groundwater potential zones were conducted using the seismoelectric surface geophysical method, existing springs, and static groundwater level data. The different stages are discussed in the following sections:

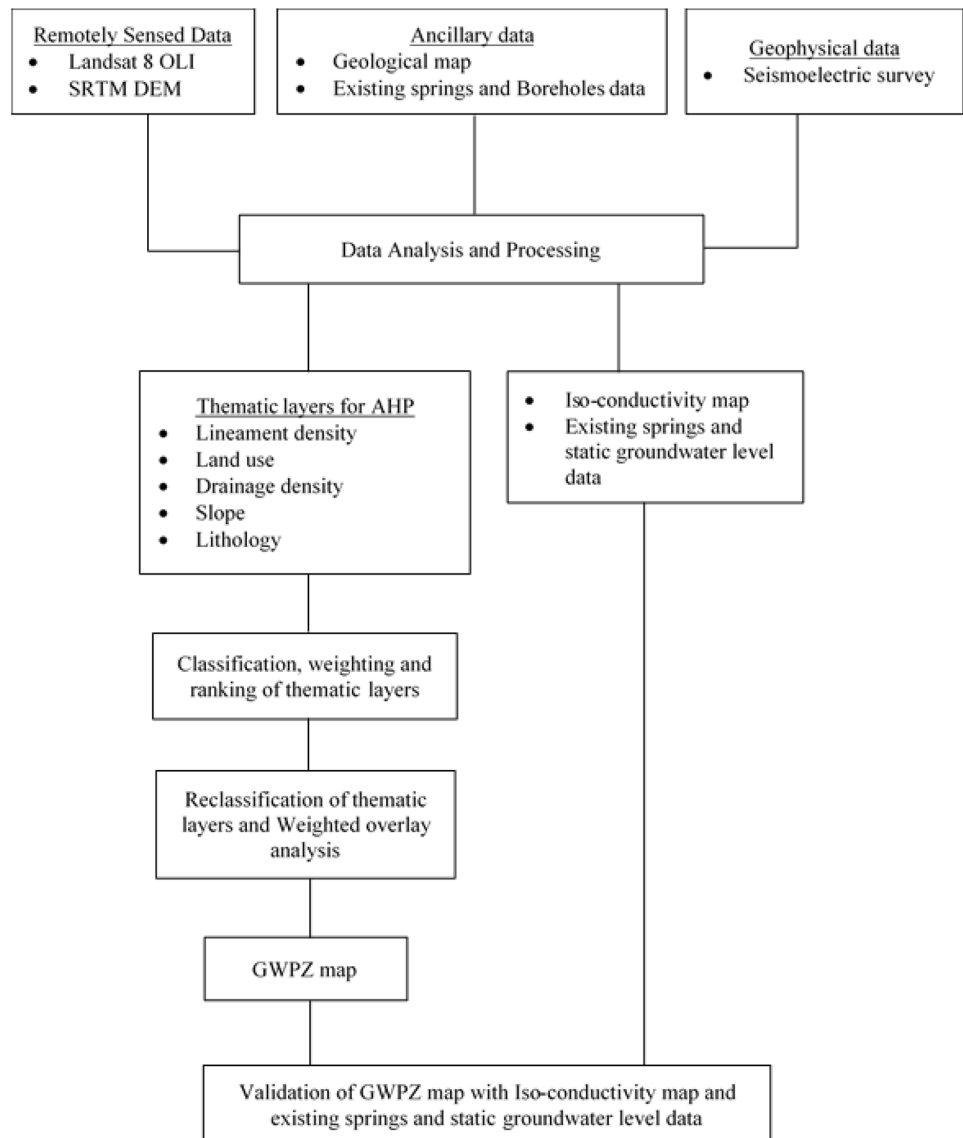
### 3.1 Geospatial techniques

Geospatial techniques were used to delineate the different groundwater potential zones. The steps used in achieving this were: (1) identifying and mapping the different surface factors that are believed to control the recharge, runoff, occurrence, and storage of groundwater; (2) reclassification of each factor with respect to its influence on recharge; (3) assigning each thematic layer

a rank and weight based on its relative importance to groundwater recharge; and finally, (4) integrating all the thematic maps in ArcGIS Pro using the weighted overlay method to generate the GWPZ map [10].

Five factors that include lithology, slope, lineament density, drainage density, and land use were used in this study. The slope and drainage density thematic maps were produced from SRTM DEM data with 30 m spatial resolution (SRTM1N04E009V3) using ArcGIS Pro. Lineament density and land use thematic maps were generated from band 7 of Landsat 8 OLI data (LC08\_L1TP\_187057\_20170507\_20170515\_01\_T1) that covers the study area [32], using ArcGIS Pro. The slope, drainage, and lineament densities were generated using the Spatial Analyst Tools, while the land use map was created using the Image Classification Tools of ArcGIS Pro. The lithology

Fig. 2 Flow chart for the methods used to carry out this study



map was reproduced from the geological map of Mount Cameroon after Ateba et al. (2009).

Lineament extraction to produce the lineament density map is a rigorous process that involves pre-processing, image enhancement, and image transformation of the Landsat 8 multispectral images using ENVI and PCI Geomatica software [33, 34]. Pre-processing involves radiometric correction (i.e., Radiometric Calibration and FLAASH Atmospheric Correction) and data resizing to the area of interest. Image enhancement involves Spectral Enhancement and Spatial Filtering using a Directional Convolution Filter. Image transformation involves Image Sharpening using Gram\_Schmidt Pan sharpening, Principal Component Analysis, Minimum Noise Fraction (MNF), and Independent Component Analysis [34, 35]. The lineaments were then extracted from the processed band 7 images using an automatic method [34, 36], with PCI Geomatica Banff. The Landsat image is processed to increase the qualities of tones and hues, image textures, lineaments, and their trends [33]. Lineaments here represent fractures, joints, and faults that act as pathways for water infiltration and groundwater flow.

### 3.2 Analytic hierarchy process (AHP)

To avoid errors and preserve the geometric properties of the data imagery, all the thematic layers were harmonised and projected onto a common Universal Transverse Mercator (UTM) coordinate system (WGS84 Zone 32 N) at 30 m resolution. The five thematic maps produced from the above-mentioned processes were used as the five factors to generate the GWPZ map using the AHP. The AHP is a multi-criteria decision-making technique originally developed by Prof. Thomas Saaty [37]. It relies on weights calculation by finding the dominant right eigenvector of a positive reciprocal decision matrix based on pairwise comparison inputs and using the fundamental scale of values to represent the intensities of importance [37, 38]. Using the Analytic Hierarchy Process Online Software (AHP-OS) developed by Klaus Goepel, the five criteria (factors) were used for the pairwise comparison (*pwc*), based on the equations below [38].

$$pwc = (a_1, a_2 \dots a_{npc}), (x_1, x_2, \dots x_{npc}) \quad (1)$$

With integers  $a_i \in [0, 1]$ ,  $x_i \in [1, M]$ ,  $M=9$  and  $i=1 \dots npc$ , where *npc* is the number of pairwise comparisons and *M* is the decision matrix. For *n* criteria, the  $n \times n$  decision matrix is then filled from *pwc*.

$$npc = \frac{n^2 - n}{2} \quad (2)$$

The five influencing factors with their weighted percentages were geoprocesed using Weighted Overlay under the Spatial Analyst Tools of ArcGIS Pro to generate the GWPZ map. All the input criteria were reclassified to integer rasters before they were used in Weighted Overlay. An output scale value of 1–5 selected from the Scale setting was used to assign scale values for the criteria after setting the Evaluation Scale at 1–5, where 1 represents the lowest and 5 is the most favourable for groundwater recharge and occurrence.

### 3.3 Verification and validation

Validation and field verification of the GWPZ map were carried out via surface geophysical surveys using the seismoelectric method and investigating the existing springs and static water levels.

The seismoelectric method involves the propagation of a seismic wave in a medium that induces an electrical field or causes the radiation of an electromagnetic wave [39]. Hence, the seismoelectric method involves the use of a seismic source and electric or magnetic field receivers. The ATS GeoSuite app was used as the receiver, while a sledgehammer generated the seismic wave. Sounding was done on 253 points spread over the study area. The data were collected during the dry season to avoid seasonal aquifers and raised water tables due to infiltration from rainwater. It was entered into an Excel sheet, which was added to ArcGIS Pro, and then inserted into the geostatistical kriging method for interpolation to produce an iso-conductivity map of the study area that was used as field verification and validation of the GWPZ.

Other means of validation used are existing springs and the static water level in boreholes. Data from 240 producing boreholes, 10 dry boreholes, and 19 springs were used to validate the GWPZ.

## 4 Results and interpretation

The results obtained on various aspects, namely lithology, land use, lineament density, drainage density, slope, seismoelectric survey, existing springs, and static water levels are discussed below.

### 4.1 Factors influencing groundwater recharge

#### 4.1.1 Lithology

Lithology is the most important factor controlling groundwater recharge and occurrence in the study area (Table 1). For groundwater to be stored in aquifers, there must exist suitable lithological conduits for infiltration

and groundwater flow. These conduits are provided by the presence of fractures and the high primary porosity of pyroclastic rocks, which increases with age. The lithology of Buea is made of basanites, lahars, trachytes, and trachybasalts of different ages (Fig. 3). These rocks occur as alternate layers of lava flow and pyroclastic rocks. The oldest basanites and trachytes/trachybasalts occur in the central and southeastern parts of the study area and divide the younger rocks in the north and southwest. The recent rocks can be found in the northwest, ascending Mount Cameroon. Based mainly on permeability, the rocks were reclassified and then ranked according to their influence on groundwater recharge (Table 1).

### 4.1.2 Slope

Slope is one of the main factors that influence the recharge of aquifers in terms of surface water infiltration and runoff. It is measured in degrees. The degree of slope determines whether a zone favours infiltration due to high residence time or runoff [11]. The steeper the slope, the higher the runoff and the lesser the infiltration of surface water. The steepest slopes occur in the western part, at the highest elevation. These slopes of greater than 19.00° have very low infiltration and cover about 1/5 of the total

surface area of the study area (Fig. 4a). More than half of the study area is characterised by gentle slopes of less than 9.00°. The slope map is subdivided into five slope classes; 0.00–3.73°, 3.74–5.11°, 5.12–8.84°, 8.85°–18.90°, 19.00°–45.80°, and further reclassified into very low, low, moderate, high, and very high (Table 1).

### 4.1.3 Land use

Land use is the least influential factor affecting groundwater recharge in this study (Table 1). Nonetheless, it is a significant factor affecting the groundwater recharge process [40]. The land use includes built-up or developed areas, forest, herbaceous, and cultivated areas (Fig. 4b), classified using supervised classification on the composite image of band 423. The reclassified and ranked land use is shown in Table 1. More than 50% of the study area is dominated by cultivated and herbaceous land. Cultivated and herbaceous land have the most effect on surface water infiltration into aquifers by increasing the infiltration rate. The forest zone has a thick canopy and occurs on steep slopes, thus reducing surface water percolation. Built-up and developed areas create a compacted terrain that seals the ground surface, thus preventing or reducing groundwater recharge.

**Table 1** Class ranking and percentage of thematic weight [12]

Factor/criterion (units)	Class/value range	Rating	Reclassified value	Scale/rank	Weight/priority
Lithology	Younger basalts1	1	1	3	33.2
	Recent basalts		2	1	
	Younger basalts2		3	3	
	Older basalts		4	5	
Slope (°)	0.00000728–3.73	2	1	5	30.5
	3.74–5.11		2	5	
	5.12–8.84		3	4	
	8.85°–18.9		4	2	
	19°–45.8		5	1	
Lineament density (km/km <sup>2</sup> )	Very low	3	1	3	18.4
	Low		2	3	
	Moderate		3	4	
	High		4	5	
	Very high		5	5	
Drainage density (km/km <sup>2</sup> )	Very low	4	1	5	10.9
	Low		2	5	
	Moderate		3	4	
	High		4	3	
	Very high		5	2	
Land use	Build up/Developed	5	1	3	7.0
	Forest		2	1	
	Herbaceous		3	3	
	Planted/Cultivated		4	4	

**Fig. 3** Lithology map of the study area

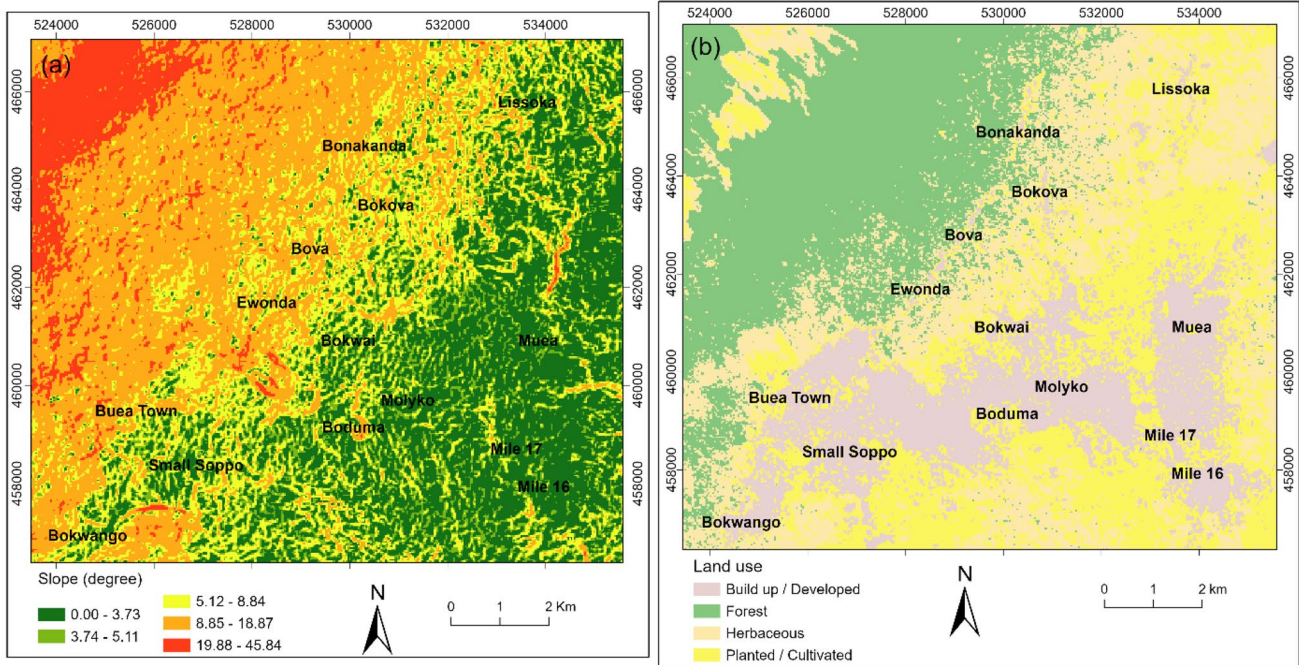
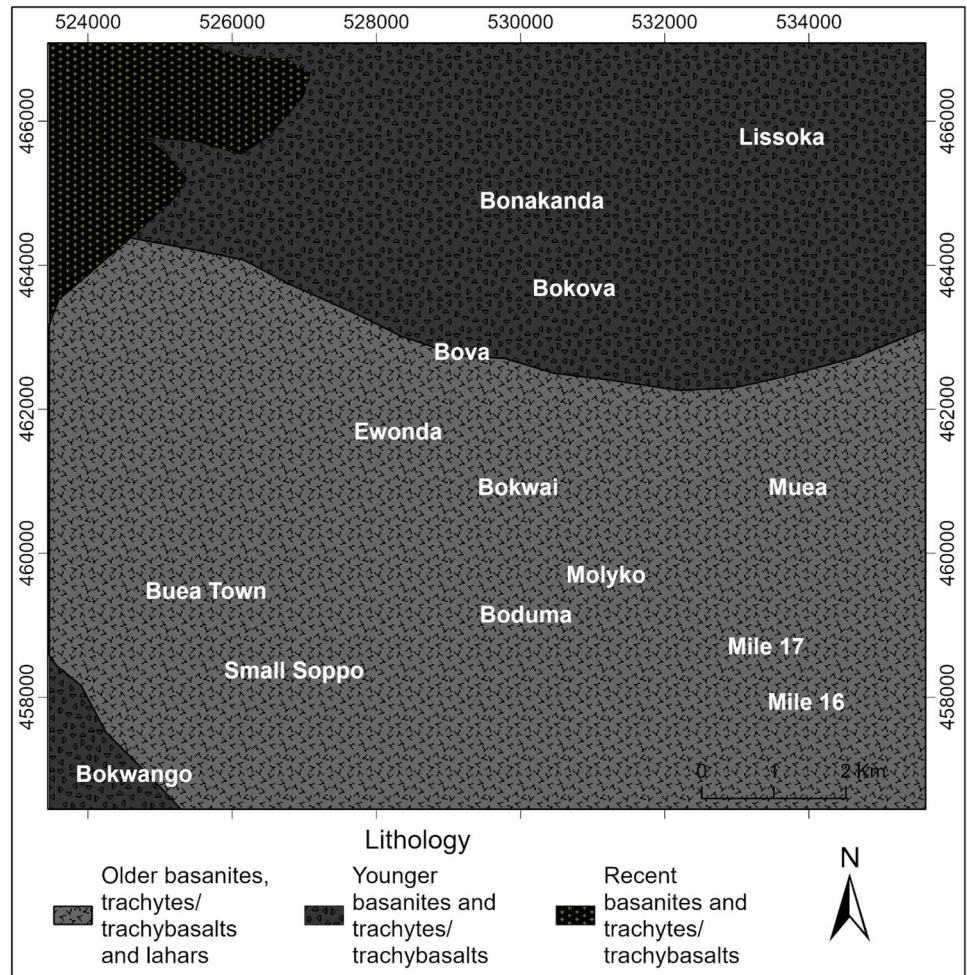


**Fig. 4** **a** Slope map of the study area, **b** Land use map of the study area

### 4.1.4 Lineament density

Lineament density is the total length of linear features per unit area [41]. The greater the amount of lineament concentration and extension in an area, the greater the lineament density, and the greater the lineament density, the higher the probability of groundwater recharge. Lineaments here may represent surface expressions of faults, folds, fractures, lithological boundaries, or rock contacts through which surface water could percolate or groundwater could flow. The study area has a high lineament density (Fig. 5a). The highest lineament density occurs in Mile 16, Mile 17, Molyko, Small Soppo, Buea Town, Lissoka, and between Bokova and Bonakanda. The northwest of Ewonda, Bova, and Bonakanda show the lack of lineament. High lineament density zones are areas of high infiltration and recharge. The high lineament density zones were ranked the highest on a scale of 5, while the low lineament density zones were given ranks of 3 (Table 1).

### 4.1.5 Drainage density

Drainage density is the ratio of the overall length of channels per unit of area [42]. The drainage pattern in the study area is dendritic, with most of the drainage originating from the mountain and highlands in the west (Fig. 5b). The drainage density is measured in km/km<sup>2</sup> and varies from 11.54 to 96.81 km/km<sup>2</sup>. Drainage

reduces infiltration due to runoff. The low drainage density areas are positive for high infiltration rates, whereas the high drainage density areas are characterised by low infiltration rates. Low drainage density zones are found in the eastern lowlands and gentle slopes of the study area. The drainage density map was reclassified into five categories: very low, low, moderate, high, and very high (Table 1).

## 4.2 Groundwater potential zonation

The groundwater potential zones of the study area were delineated by integrating lithology, drainage density, slope, lineament density, and land use thematic maps using geospatial techniques. The resulting weights for the influencing factors based on 10 pairwise comparisons by the AHP-OS are presented in Table 2. Figure 6 shows the bar chart of the resulting weights and their percentage error. The resulting weights are based on the principal eigenvector of the decision matrix below (Table 3). Through the weighted overlay technique, five groundwater potential zones were delineated: very good, good, moderate, poor, and very poor (Fig. 7). From the groundwater potential zones map, the best (very good) groundwater potential zone is concentrated in the southeastern part of the study area, whereas the northwestern region has the poorest groundwater potential. Large parts of the

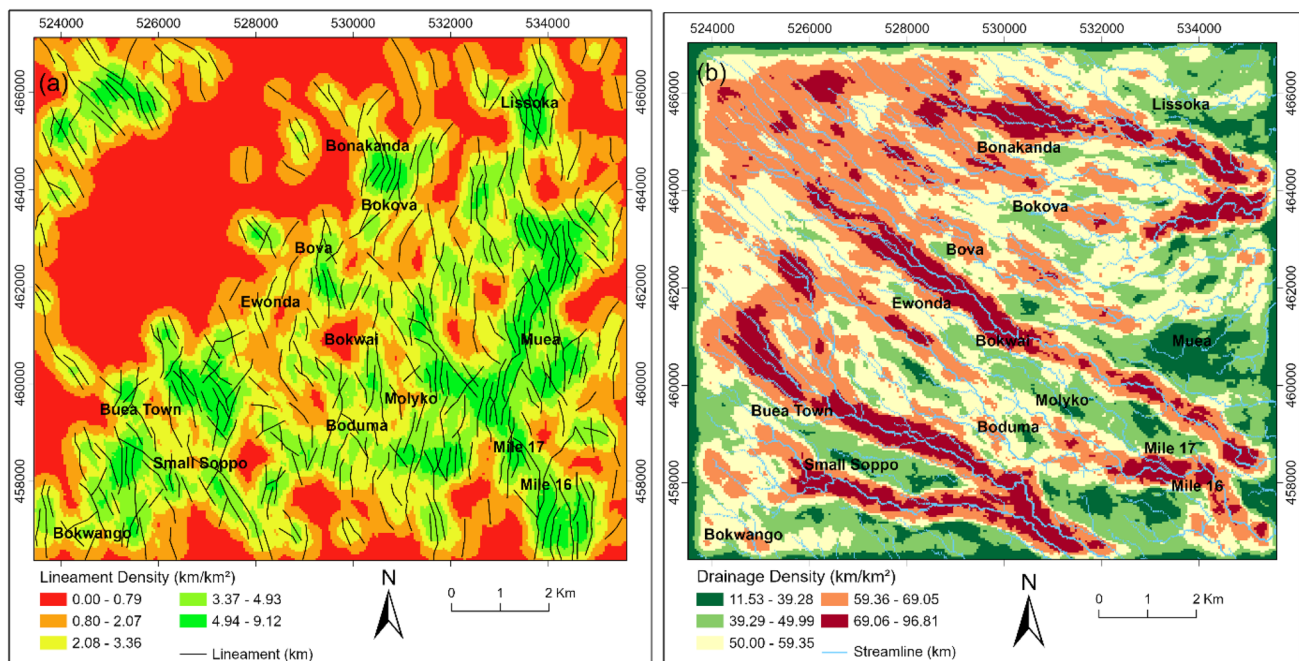


Fig. 5 a Lineament density map of the study area, b Drainage density map of the study area



**Table 2** Resulting weights for the five factors based on 10 pairwise comparisons

Factor	Weight (%)	Rank
Lithology	33.2	1
Slope	30.5	2
Lineament density	18.4	3
Drainage density	10.9	4
Land use	7.0	5

Consistency Ratio CR= 1.4%

study area fall within the good and very good groundwater potential zones.

### 4.3 Model validation

#### 4.3.1 Seismoelectric survey

The results of the 1D seismoelectric grid survey of the study area are presented in Fig. 8. There is great variability in the conductivity of the formations between 40 and 60 m below the surface. Bonakanda, Bova and the northwestern zone of the map show very low conductivity. Most of the study area is composed of moderate to high formation conductivity. High conductivity implies a high electrical conductance of the medium due to the presence of water. The highest conductivities were registered in Mile 16, Mile 17, Muea, and Molyko in the southeast.

**Fig. 6** Bar chart of the resulting weights of the five factors and their percentage errors

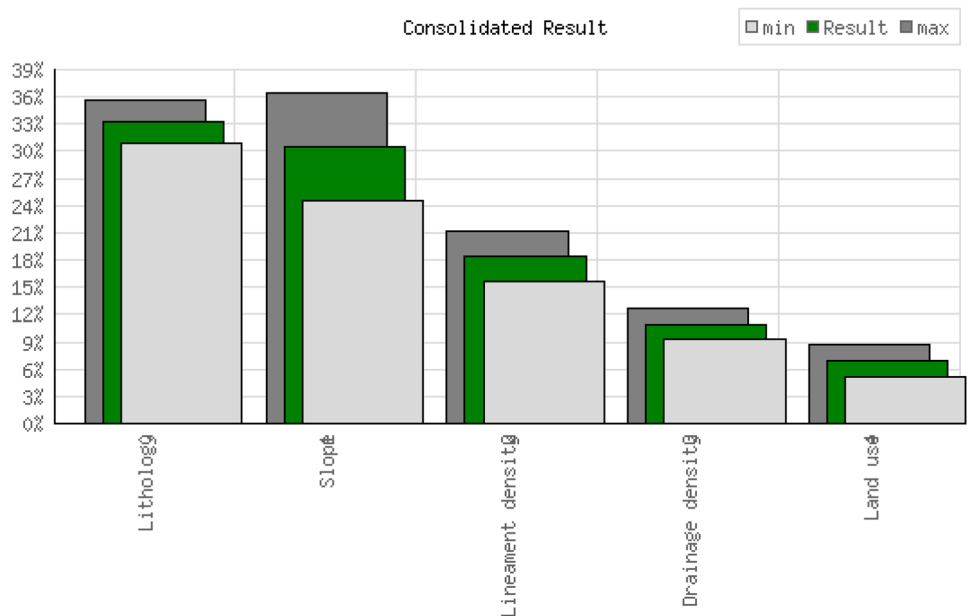


**Table 3** Decision matrix

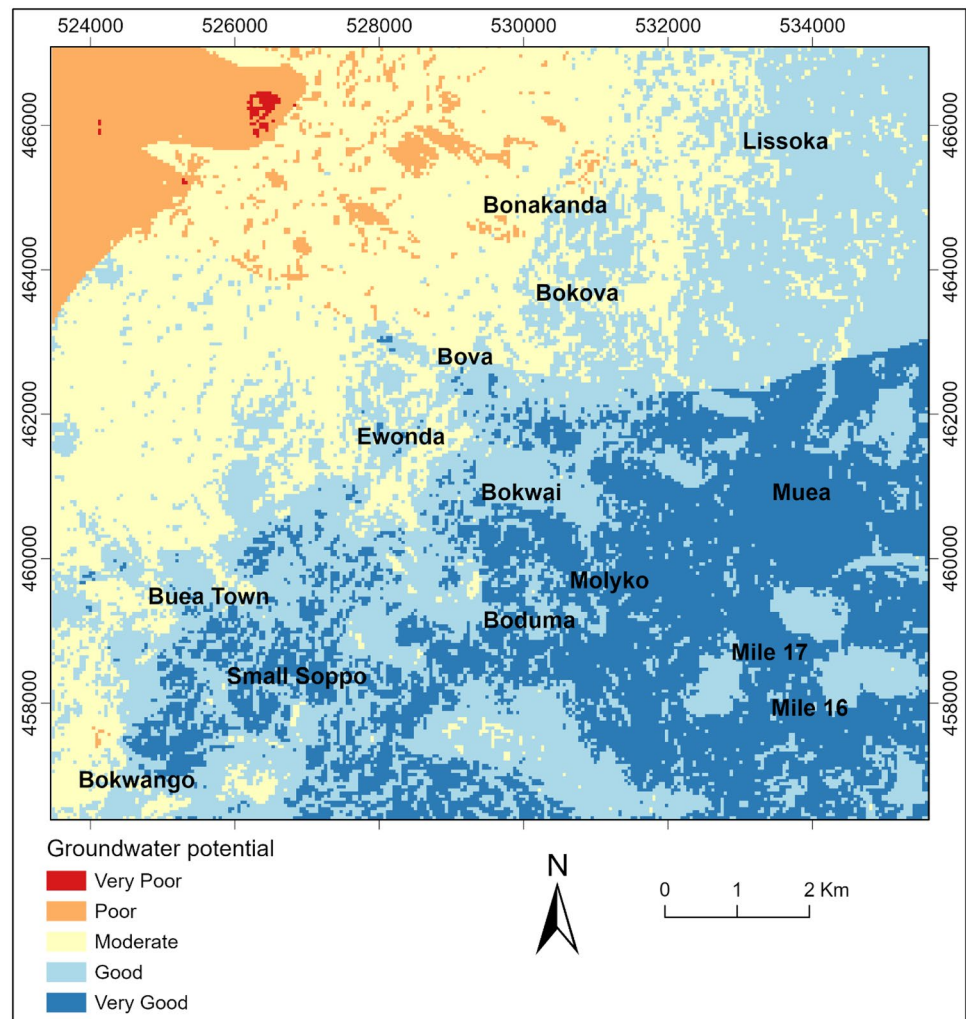
	Lithology	Slope	Lineament density	Drainage density	Land use
Lithology	1	1.00	2.00	3.00	5.00
Slope	1.00	1	2.00	3.00	3.00
Lineament density	0.50	0.50	1	2.00	3.00
Drainage density	0.33	0.33	0.50	1	2.00
Land use	0.20	0.33	0.33	0.50	1

Principal eigen value=5.062, Eigenvector solution: 4 iterations, delta=4.5E-9

#### 4.3.2 Existing springs and static water level

The existing boreholes in the study area were mapped, and their static water levels were used in validating the groundwater potential zones map. The study area has a lot of producing boreholes, the majority of which occur in very good groundwater potential zones (Fig. 9). The static water level in the boreholes varies considerably, from 10 m in the very good groundwater potential zone to 80 m in the good to moderate zones. Springs only occur in the very good groundwater zone, particularly where the groundwater table is low (10–40 m below the surface). Dry boreholes occur generally in the moderate groundwater potential zone at Bova, Bonakanda, and Bokova. These holes range from 60 to 110 m deep.

**Fig. 7** Groundwater potentiality map showing the groundwater potential zones of the study area



## 5 Discussion

### 5.1 Groundwater potential zones

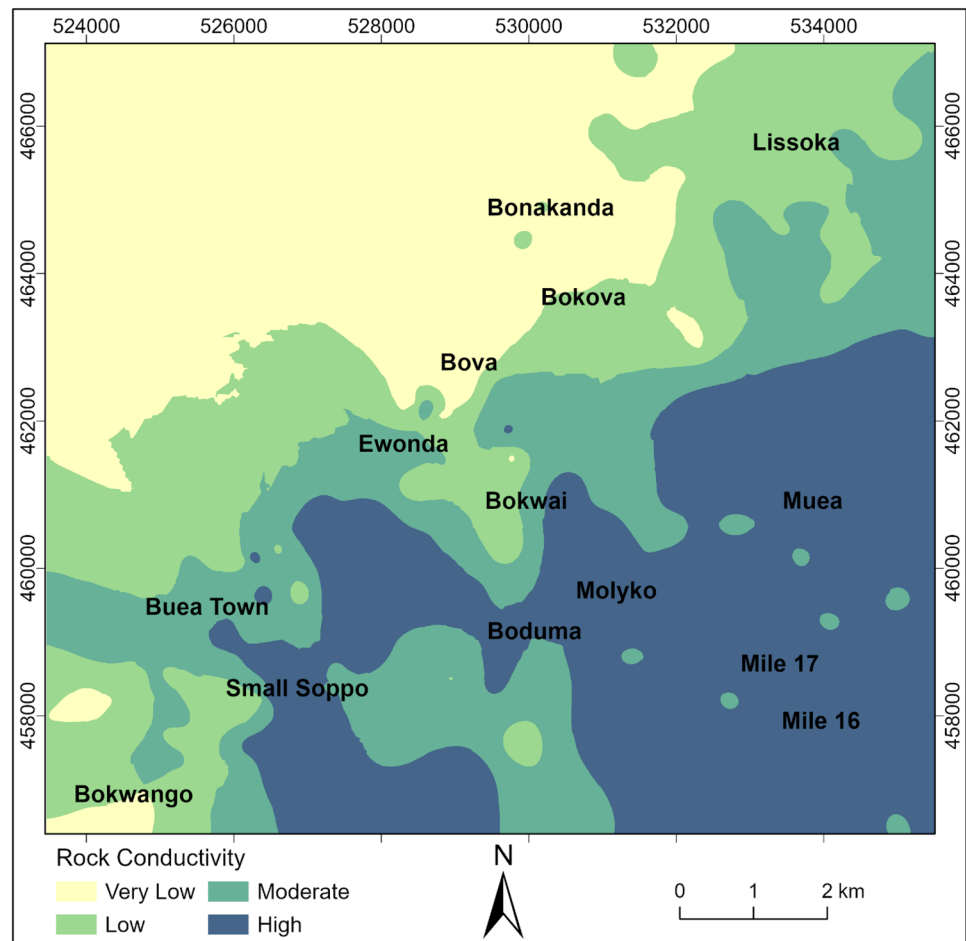
The five thematic maps that were integrated to generate the GWPZ map have different degrees of influence on aquifer recharge and thus groundwater occurrence and distribution potential, as demonstrated in similar studies [10, 11, 15, 40]. The weighted thematic maps have a consistency ratio of 1.4% (0.014) (see Table 2), implying the reasoning of the AHP is consistent [15, 18], and the GWPZ map is reliable. The influencing attributes under lithology, slope, lineament density, drainage density, and land use have varied groundwater potentials classified as very poor to very good (Table 4). The importance of each thematic layer to groundwater recharge and occurrence is further discussed.

Low slope angles, high lineament densities, low drainage densities, herbaceous and cultivated land, and the older permeable basanites epitomise good to very good

groundwater potential zones in the study area (Table 4). On the other hand, poor groundwater potential zones are typified by high slope, low lineament density (little or no surface lineaments), high drainage density, forest, and recent basanites. Large parts of the study area fall within the good and very good groundwater potential zones. This is mainly due to the geological nature of the terrain, which consists of lahars and old weathered and fractured basanites of high permeability, a similar situation noted by Serele et al. [20] in Madagascar. Geology (lithology and fractures) and topography also play major roles in infiltration and runoff [43]. Hence, the influence of land use on groundwater recharge is dependent on the underlying geologic conditions and the topography [44], other than manmade structures. This explains why we have high groundwater potential in built-up and developed areas, even though these areas are characterised by low infiltration and high runoff.

The ability of formations to host groundwater depends on some geologic factors like rock age,

**Fig. 8** Iso-conductivity map of study area as per 1D seismic-electric survey



fracturing, and unconformity, all of which influence infiltration, percolation, and groundwater flow. Age increases the porosity of hard rocks as they become more porous and permeable due to weathering and deformation. These elucidate why the older basanites zone has the greatest groundwater potential (Fig. 7 and Table 4). Fracturing results in secondary porosity and permeability. Thus, high lineament density in the study area might be revealing of secondary porosity and permeability represented by fracture systems serving as conduits for the movement and storage of groundwater [12].

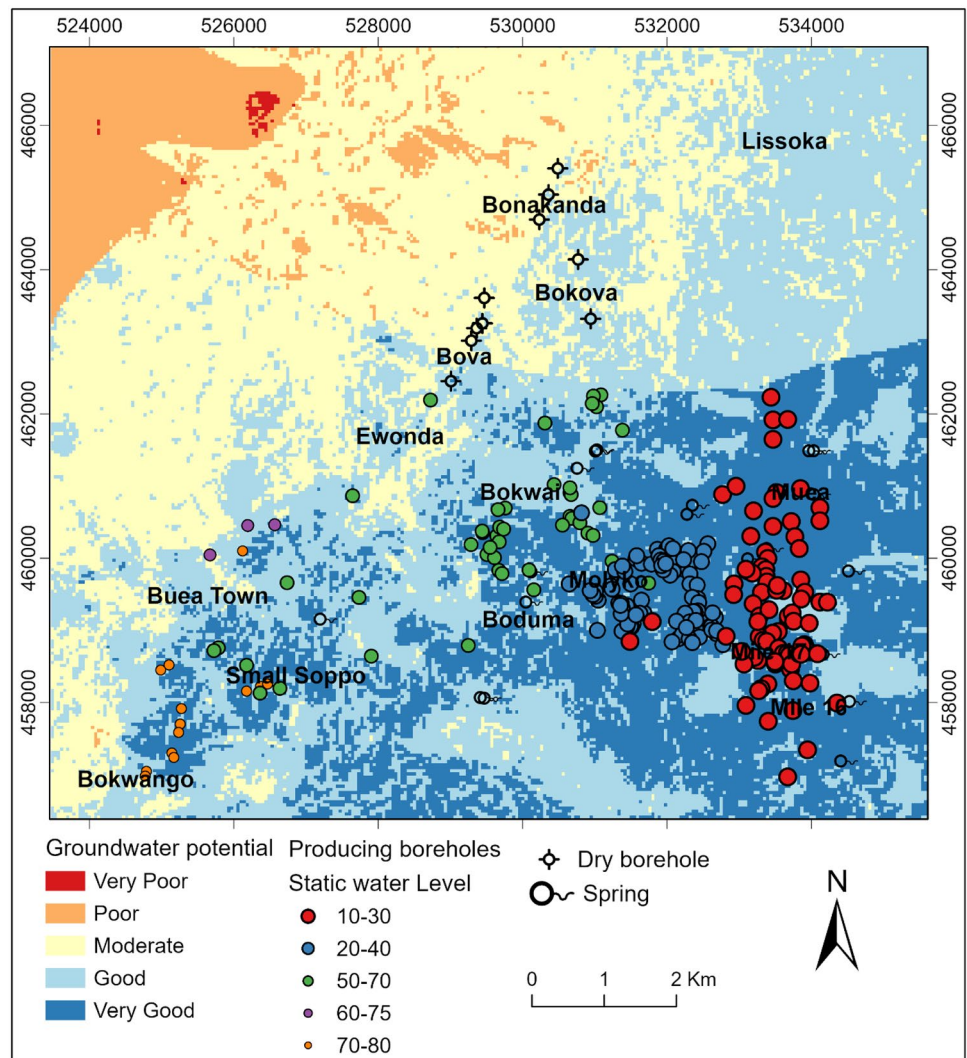
Slope has an inverse relationship with infiltration but a direct proportionality with runoff because surface runoff is low on gentle slopes and plains, allowing more time for surface water infiltration into the subsurface and vice versa [8, 16, 44]. Gentle slopes in the eastern part of the study area have good to very good groundwater potential (Fig. 7 and Table 4). Similarly, low drainage density, which is associated with gentle slopes, favours reduced runoff, increased infiltration and good groundwater recharge [16, 40].

## 5.2 Validation of the groundwater potential zones map

Validation of groundwater potential zone maps using surface geophysics and borehole yield data has been carried out successfully elsewhere [11, 13]. The correlation of the GWPZ map with the seismic-electric (iso-conductivity) map gives agreeable results. The iso-conductivity map (Fig. 8) highlights the very good groundwater potentiality of the southeastern part of the study area and the poor groundwater potentiality of the northwestern part (Fig. 7). It shows that the poor groundwater potential zone has very high apparent resistivity (low conductivity) and further confirms that the reason for the dry holes in Bova, Bonakanda, and Bokova is due to the very low conductivity of the formations. The very low conductivity implies no or little groundwater in this region. Low lineament density, high drainage density, young basanites, and steep slopes are also characteristic of this zone.

After the correlation between the groundwater potential zones map and the iso-conductivity map, additional validation was done by overlaying existing springs, boreholes,

**Fig. 9** Validated groundwater potential map of study area



and static water level data on the GWPZ map (Fig. 9). Understanding the spatial distribution of existing springs and the static groundwater level is very important in understanding the groundwater resource distribution [13]. The reported static water level and spring data show a good correlation with the groundwater potential zones and iso-conductivity map. Springs are an expression of subterranean flow processes that are otherwise accessible only through boreholes. Springs are common in volcanic terrain, particularly in lowland areas. All the springs in the study area occur in the older basanite formation at lower altitudes and gentle slopes within the “very good” groundwater potential zones with high formation conductivity. Almost all the productive boreholes fall within the very good groundwater potential zone in the built-up area and on gentle slopes. The concentration of boreholes in the built-up area is an obvious sign of the high demand for water for human activities. From the groundwater potential zones map, it is evident that all boreholes with a static water level of 10–40 m are in the

“very good” zone, whereas the dry boreholes occur in the “moderate to poor” zone with high resistivity (very low conductivity). This high resistivity zone also correlates with the occurrence of younger volcanic rocks. This further confirms that mainly the geological setting controls the occurrence of dry and producing boreholes, since all dry boreholes occur in the younger basanites and trachytes/trachybasalts zone, which also displays gentle slopes, low drainage density, high lineament density, and cultivated and herbaceous land. Another notable observation is that as we move from the “very good” to “poor” zones, which also correspond to gentle slopes to steep slopes, the static water level drops deeper.

## 6 Conclusions

This study displays the efficiency of employing an integrated approach of remote sensing, geophysical, existing springs, and static water level data in prospecting for

**Table 4** Classification of groundwater potentiality of thematic layers

Factors	Attributes	Groundwater potential
Lithology	Younger basalts	Moderate to good
	Recent basalts	Poor to very poor
	Older basalts	Good to very good
Slope	Gentle sloping	Very good
	Moderate sloping	Good
	Moderate to steep sloping	Moderate
	Steep sloping	Moderate to poor
	Very steeply sloping	Poor
Lineament density	Very low	Poor
	Low	Moderate
	Moderate	Good
	High	Good to very good
	Very high	Very good
Drainage density	Very low	Very good
	Low	Good
	Moderate	Moderate
	High	Poor
	Very high	Very poor
Land use	Build up/Developed	Moderate
	Forest	Poor
	Herbaceous	Good
	Planted/Cultivated	Very good

groundwater in volcanic terrain. Employing geospatial techniques, five groundwater potential zones were determined using five primary groundwater recharge controlling parameters that include lithology, slope, drainage density, lineament density, and land use. An iso-conductivity map used to verify the GWPZ map highlighted four groundwater potential zones, which are in strong correlation with those on the GWPZ map. More than half of the study area falls in the "good" to "very good" zones, indicating most of the study area has good groundwater potential. These results were validated by existing springs and static water level data overlays. The spatial distribution of the existing springs and the static water level is in close agreement with the GWPZ and iso-conductivity maps. The moderate groundwater potential zone, the very low conductivity zone, the geology of the terrain, the absence of springs, and the dry boreholes explain the scarcity in water supply being experienced in Bova, Bonakanda, and Bokova. The final map can be used to increase the success ratio of installing groundwater boreholes and as a guide for decision-making regarding sustainable groundwater development and management.

This integrated approach for groundwater prospecting is recommended in both urban and remote areas in order

to obtain effective results. Furthermore, due to the higher cost of geophysical surveys, it is also recommended that remote sensing and geospatial techniques be used as a time- and cost-effective approach to selecting sites for field geophysical surveys before drilling boreholes.

**Author contributions** All authors contributed to the study's conception and design. Material preparation, data collection, and analysis were performed by LJNN. LJNN wrote the first draft of the manuscript, while AEDL and CMA revised it critically for important intellectual content. All authors read and approved the final manuscript and agreed to be accountable for all aspects of the work.

**Funding** The authors declare that no funds, grants, scholarships, or other supports were received during this research.

**Data availability** The Landsat 8 and SRTM data are available at <https://earthexplorer.usgs.gov/>. The shapefiles, borehole, and geophysical data generated during and/or analysed during the current study are available from the corresponding author on reasonable request.

## Declarations

**Conflict of interest** The authors have no competing interests to declare that are relevant to the content of this article.

**Open Access** This article is licensed under a Creative Commons Attribution 4.0 International License, which permits use, sharing, adaptation, distribution and reproduction in any medium or format, as long as you give appropriate credit to the original author(s) and the source, provide a link to the Creative Commons licence, and indicate if changes were made. The images or other third party material in this article are included in the article's Creative Commons licence, unless indicated otherwise in a credit line to the material. If material is not included in the article's Creative Commons licence and your intended use is not permitted by statutory regulation or exceeds the permitted use, you will need to obtain permission directly from the copyright holder. To view a copy of this licence, visit <http://creativecommons.org/licenses/by/4.0/>.

## References

- Ott W (2014) Access to drinking water and stakeholder action—drinking water governance in Cameroon from a political-ecological perspective case study: upper Mefou watershed, Cameroon. Master Thesis, Freie Universität Berlin
- Emile R, Clammer JR, Jayaswal P, Sharma P (2022) Addressing water scarcity in developing country contexts: a socio-cultural approach. *Humanit Soc Sci Commun*. <https://doi.org/10.1057/s41599-022-01140-5>
- Gadgil A (1998) Drinking water in developing countries. *Annu Rev Energy Env* 23(1):253–286. <https://doi.org/10.1146/annurev.energy.23.1.253>
- Chakkaravarthy DN (2019) Water scarcity-challenging the future. *Int J Agric Environ Biotechnol*. <https://doi.org/10.30954/0974-1712.08.2019.2>
- Gleeson T, Befus KM, Jasechko S, Luijendijk E, Cardenas MB (2016) The global volume and distribution of modern

- groundwater. *Nat Geosci* 9(2):161–164. <https://doi.org/10.1038/ngeo2590>
6. Richts A, Struckmeier WF, Zaepke M (2011) WHYMAP and the groundwater resources map of the world 1: 25,000,000. *Sustain Groundw Resour*. [https://doi.org/10.1007/978-90-481-3426-7\\_10](https://doi.org/10.1007/978-90-481-3426-7_10)
  7. Fan Y, Li H, Miguez-Macho G (2013) Global patterns of groundwater table depth. *Science* (1979) 339(6122):940–943. <https://doi.org/10.1126/science.1229881>
  8. Serele C, Pérez-Hoyos A, Kayitakire F (2020) Mapping of groundwater potential zones in the drought-prone areas of south Madagascar using geospatial techniques. *Geosci Front* 11(4):1403–1413. <https://doi.org/10.1016/j.gsf.2019.11.012>
  9. Tafila O, Ranganai RT, Moalafhi DB, Moreri KK, Maphanyane JG (2022) Investigating groundwater recharge potential of Notwane catchment in Botswana using geophysical and geospatial tools. *J Hydrol Reg Stud*. <https://doi.org/10.1016/j.ejrh.2022.101011>
  10. Gaber A, Mohamed AK, Elgalladi A, Abdelkareem M, Beshr AM, Koch M (2020) Mapping the groundwater potentiality of West Qena area, Egypt, using integrated remote sensing and hydro-geophysical techniques. *Remote Sens (Basel)*. <https://doi.org/10.3390/rs12101559>
  11. Ishola KS, Fatoyinbo AA, Hamid-Mosaku AI, Okolie CJ, Daramola OE, Lawal TO (2023) Groundwater potential mapping in hard rock terrain using remote sensing, geospatial and aeromagnetic data. *Geosyst Geoenviron* 2(1):100107. <https://doi.org/10.1016/j.geogeo.2022.100107>
  12. Thapa R, Gupta S, Guin S, Kaur H (2017) Assessment of groundwater potential zones using multi-influencing factor (MIF) and GIS: a case study from Birbhum district, West Bengal. *Appl Water Sci* 7(7):4117–4131. <https://doi.org/10.1007/s13201-017-0571-z>
  13. Amer R, Sultan M, Ripperdan R, Ghulam A, Kusky T (2013) An integrated approach for groundwater potential zoning in shallow fracture zone aquifers. *Int J Remote Sens* 34(19):6539–6561. <https://doi.org/10.1080/01431161.2013.804221>
  14. Magaia LA, Goto T, Masoud AA, Koike K (2017) Identifying groundwater potential in crystalline basement rocks using remote sensing and electromagnetic sounding techniques in central western Mozambique. *Nat Resour Res*. <https://doi.org/10.1007/s11053-017-9360-5>
  15. Echogdali FZ et al (2022) Application of analytical hierarchy process and geophysical method for groundwater potential mapping in the Tata basin, Morocco. *Water (Switzerland)*. <https://doi.org/10.3390/w14152393>
  16. Prasad RK, Mondal NC, Banerjee P, Nandakumar MV, Singh VS (2008) Deciphering potential groundwater zone in hard rock through the application of GIS. *Environ Geol* 55(3):467–475. <https://doi.org/10.1007/s00254-007-0992-3>
  17. Magesh NS, Chandrasekar N, Soundranayagam JP (2012) Delineation of groundwater potential zones in Theni district, Tamil Nadu, using remote sensing, GIS and MIF techniques. *Geosci Front* 3(2):189–196. <https://doi.org/10.1016/j.gsf.2011.10.007>
  18. Shebl A, Abdelaziz MI, Ghazala H, Araffa SAS, Abdellatif M, Csámer Á (2022) Multi-criteria ground water potentiality mapping utilizing remote sensing and geophysical data: a case study within Sinai Peninsula, Egypt. *Egypt J Remote Sens Sp Sci* 25(3):765–778. <https://doi.org/10.1016/j.ejrs.2022.07.002>
  19. Yossa MT, Lordon AED, Agyingi CM, Agbor-Taku J, Shandini YN, Bessong CE (2023) Remote sensing and geographic information system (GIS)-based high-resolution mapping of potential groundwater recharge zones on the hard rock terrains of the Cameroon volcanic line (CVL). *SN Appl Sci*. <https://doi.org/10.1007/s42452-022-05248-w>
  20. Njome MS, Suh CE, Sparks RSJ, Ayonghe SN, Fitton JG (2008) The Mount Cameroon 1959 compound lava flow field: morphology, petrography and geochemistry. *Swiss J Geosci* 101(1):85–98. <https://doi.org/10.1007/s00015-007-1245-x>
  21. Olivry JC (1986) Fleuves et rivières du cameroun, pp 15–17. Accessed 13 Mar 2023. [Online]. Available: [https://books.google.com/books/about/Fleuves\\_et\\_rivi%C3%A8res\\_du\\_Cameroun.html?hl=fr&id=XqJWAAAAMAAJ](https://books.google.com/books/about/Fleuves_et_rivi%C3%A8res_du_Cameroun.html?hl=fr&id=XqJWAAAAMAAJ)
  22. Climate & Weather Averages in Buea, Cameroon. <https://www.timeanddate.com/weather/@2233410/climate>. Accessed 18 Jul 2023
  23. Molua EL, Lambi CM (2006) Climate hydrology and water resources in Cameroon, p 37. [https://doi.org/10.1007/978-94-009-0207-7\\_1](https://doi.org/10.1007/978-94-009-0207-7_1)
  24. Suh CE et al (2003) The 1999 and 2000 eruptions of Mount Cameroon: eruption behaviour and petrochemistry of lava. *Bull Volcanol* 65(4):267–281. <https://doi.org/10.1007/s00445-002-0257-7>
  25. Ateba B et al (2009) Eruptive and earthquake activities related to the 2000 eruption of Mount Cameroon volcano (West Africa). *J Volcanol Geoth Res* 179(3–4):206–216. <https://doi.org/10.1016/j.jvolgeores.2008.11.021>
  26. Fairhead JD, Okereke CS (1987) A regional gravity study of the West African rift system in Nigeria and Cameroon and its tectonic interpretation. *Tectonophysics* 143(1–3):141–159. [https://doi.org/10.1016/0040-1951\(87\)90084-9](https://doi.org/10.1016/0040-1951(87)90084-9)
  27. Stuart GW, Fairhead JD, Dorbath L, Dorbath C (1985) A seismic refraction study of the crustal structure associated with the Adamawa Plateau and Garoua Rift, Cameroon, West Africa. *Geophys J R Astron Soc* 81(1):1–12. <https://doi.org/10.1111/J.1365-246X.1985.TB01346.X>
  28. Poudjom Djomani YH, Nnange JM, Diament M, Ebinger CJ, Fairhead JD (1995) Effective elastic thickness and crustal thickness variations in west central Africa inferred from gravity data. *J Geophys Res*. <https://doi.org/10.1029/95jb01149>
  29. Fitton JG (1987) The Cameroon line, West Africa: a comparison between oceanic and continental alkaline volcanism. *Geol Soc Spec Publ* 30(May 2014):273–291. <https://doi.org/10.1144/GSL.SP.1987.030.01.13>
  30. Ateba B, Ntepe N (1997) Post-eruptive seismic activity of Mount Cameroon (Cameroon) West Africa: a statistical analysis
  31. Tsafack J-PF, Wandji P, Bardintzeff J-M, Bellon H, Guillou H, Tsafack J (2009) The Mount Cameroon stratovolcano (Cameroon Volcanic Line, Central Africa): petrology, geochemistry, isotope and age data. *Geochem Mineral Petrol* 47:65–78
  32. EarthExplorer. <https://earthexplorer.usgs.gov/>. Accessed 15 Mar 2023
  33. Gupta RP (2003) Remote sensing geology, 2nd edn. Springer-Verlag Berlin Heidelberg, New York. <https://doi.org/10.1007/978-3-662-05283-9>
  34. Farahbakhsh E et al (2020) Computer vision-based framework for extracting tectonic lineaments from optical remote sensing data. *Int J Remote Sens* 41(5):1760–1787. <https://doi.org/10.1080/01431161.2019.1674462>
  35. Getting Started with ENVI Tutorial. <https://envi.geoscene.cn/help/Subsystems/envi/Content/Tutorials/Tools/GettingStartedWithENVITutorial.htm>. Accessed 19 Mar 2023
  36. Chang YC, Song GS, Hsu SK (1998) Automatic extraction of ridge and valley axes using the profile recognition and polygon-breaking algorithm. *Comput Geosci* 24(1):83–93. [https://doi.org/10.1016/S0098-3004\(97\)00078-2](https://doi.org/10.1016/S0098-3004(97)00078-2)
  37. Saaty TL (1980) Analytic hierarchy process planning, priority setting, resource allocation. McGraw-Hill Inc, New York
  38. Goepel K (2018) Implementation of an online software tool for the analytic hierarchy process (AHP-OS). *Int J Anal Hierarchy Process* 10(3):469–487. <https://doi.org/10.13033/ijahp.v10i3.590>

39. Peng R, Wei JX, Di BR, Ding PB, Liu ZC (2016) Experimental research on seismoelectric effects in sandstone. *Appl Geophys* 13(3):425–436. <https://doi.org/10.1007/s11770-016-0570-0>
40. Ghosh PK, Bandyopadhyay S, Jana NC (2016) Mapping of groundwater potential zones in hard rock terrain using geoinformatics: a case of Kumari watershed in western part of West Bengal. *Model Earth Syst Environ*. <https://doi.org/10.1007/s40808-015-0044-z>
41. O’leary DW, Friedman JD, Pohn HA (1976) Lineament, linear, lineation: some proposed new standards for old terms. *Bull Geol Soc Am* 87(10):1463–1469. [https://doi.org/10.1130/0016-7606\(1976\)87%3c1463:LLLSPN%3e2.0.CO;2](https://doi.org/10.1130/0016-7606(1976)87%3c1463:LLLSPN%3e2.0.CO;2)
42. Tucker GE, Catani F, Rinaldo A, Bras RL (2001) Statistical analysis of drainage density from digital terrain data. *Geomorphology* 36(3–4):187–202. [https://doi.org/10.1016/S0169-555X\(00\)00056-8](https://doi.org/10.1016/S0169-555X(00)00056-8)
43. Greenbaum D (1985) Review of remote sensing applications to groundwater exploration in basement and regolith. Nottingham NG12. Accessed 01 Apr 2023. [Online]. Available: [https://nora.nerc.ac.uk/id/eprint/505150/1/WC\\_OG\\_85\\_1.pdf](https://nora.nerc.ac.uk/id/eprint/505150/1/WC_OG_85_1.pdf)
44. Omolaiye GE et al (2020) Integration of remote sensing, GIS and 2D resistivity methods in groundwater development. *Appl Water Sci*. <https://doi.org/10.1007/s13201-020-01219-x>

**Publisher’s Note** Springer Nature remains neutral with regard to jurisdictional claims in published maps and institutional affiliations.